J. Fluid Mech. (2006), *vol.* 556, *pp.* 271–282.
doi:10.1017/S0022112006009244 Printed in the United Kingdom

Large-scale motions in a supersonic turbulent boundary layer

By B. GANAPATHISUBRAMANI, N. T. CLEMENS AND D. S. DOLLING

Center for Aeromechanics Research, The University of Texas at Austin, 210 E. 24th Street, WRW220, Mail Code C0604, Austin, TX 78712, USA

(Received 14 July 2005 and in revised form 19 December 2005)

Wide-field particle image velocimetry measurements were performed in a Mach 2 turbulent boundary layer to study the characteristics of large-scale coherence at two wall-normal locations ($y/\delta = 0.16$ and 0.45). Instantaneous velocity fields at both locations indicate the presence of elongated streamwise strips of uniform low- and high-speed fluid (length $> 8\delta$). These long coherent structures exhibit strong similarities to those that have been found in incompressible boundary layers, which suggests an underlying similarity between the incompressible and supersonic regimes. Two-point correlations of streamwise velocity fluctuations show coherence over a longer streamwise distance at $y/\delta = 0.45$ than at $y/\delta = 0.16$, which indicates an increasing trend in the streamwise length scale with wall-normal location. The spanwise scale of these uniform-velocity strips increases with increasing wall-normal distance as found in subsonic boundary layers. The large-scale coherence observed is consistent with the very large-scale motion (VLSM) model proposed by Kim & Adrian (*Phys. Fluids*, vol. 11, 1999, p. 417) for incompressible boundary layers.

1. Introduction

Large-scale coherent motions are believed to play an important role in the dynamics of both subsonic and supersonic turbulent boundary layers. A broad overview on the existence of coherent structures in incompressible flows can be found in several review articles including Robinson (1991) and Panton (1997). Recently, Ganapathisubramani, Longmire & Marusic (2003) and Tomkins & Adrian (2003) performed particle image velocimetry measurements in streamwise–spanwise planes ($x-z$; in this paper x, y and z are the streamwise, wall-normal and spanwise directions respectively) and found elongated uniform low- and high-speed regions (length $> 2\delta$, δ is the boundary layer thickness). Head & Bandyopadhyay (1981) and Adrian, Meinhart & Tomkins (2000) have hypothesized that large-scale coherence is a result of individual hairpin vortices (first proposed by Theodorsen 1952) convecting as groups. Adrian *et al.* (2000) termed such a group a 'hairpin packet' (the authors noted that the term hairpin represented various types of structures including cane, horseshoe, Λ and Ω shaped individual vortices) and noted that the presence of these hairpin packets could explain the multiple ejections and sweeps found in previous hot-wire measurements and the long tails in autocorrelations (Kovasznay, Kibens & Blackwelder 1970; Bogard & Tiederman 1986).

In comparison, information on the spatial structure of supersonic boundary layers is sparse. A summary of the knowledge on organized motions in supersonic boundary

layers can be found in Smits & Dussauge (1996). Flow visualization studies by Smith & Smits (1995) in streamwise–wall-normal ($x-y$) planes of a Mach 2.9 turbulent boundary layer indicated the presence of large-scale motions qualitatively similar to the large-scale coherence found in a subsonic boundary layer by Head & Bandyopadhyay (1981). Rayleigh scattering visualization of $x-z$-planes by Smith, Smits & Miles (1989) and Smith & Smits (1995) of a Mach 2.5 boundary layer at various wall-normal locations did not reveal long streamwise structures. Smits *et al.* (1989) computed two-point correlations in a Mach 2.9 turbulent boundary layer to study the streamwise extent of large-scale motions and compared them to those measured in incompressible turbulent boundary layers. They found that the streamwise length scale of mass-flux autocorrelations in supersonic flows was about half the length scale in incompressible flows, which suggests that the large-scale motions in supersonic flows do not extend as far downstream as they do in incompressible flows. The correlation coefficient decayed to a value of 0.1 at a streamwise distance of 0.6δ at a wall-normal location $y/\delta = 0.2$. Smits *et al.* (1989) also found that the spanwise scales of the correlations in supersonic flow were similar to those in incompressible boundary layers. Both cases exhibited an increasing trend in spanwise scale with distance from the wall. Smits & Dussauge (1996) suggested that the streamwise length scales decrease significantly with increasing Mach number, whereas the spanwise scales are unaffected by the changes in Mach and Reynolds number.

In other work in compressible boundary layers, Owen & Horstmann (1972) noted that the large-scale motions in a Mach 7 boundary layer remained coherent long enough to be convected several boundary layer thicknesses downstream. Samimy, Arnette & Elliot (1994) performed Rayleigh scattering visualization experiments in streamwise–spanwise ($x-z$) planes in the outer layer ($y/\delta = 0.49$ and 0.65) of a Mach 3 boundary layer and found the presence of longitudinal streamwise structures that extend to large distances in the streamwise direction. Garg & Settles (1998) performed correlation analyses on density gradient data obtained using focusing schlieren deflectometry in a Mach 3 turbulent boundary layer to study the streamwise length scales. They found that significant correlation (correlation coefficient ≈ 0.2) was present for large separation ($\approx 2\delta$) at $y/\delta = 0.38$ indicating that structures are relatively large scale. Two-point correlations of wall-pressure measurements and Pitot pressure measurements by Ünalmis & Dolling (1998) have also shown the existence of long coherent regions (extending beyond $10\delta - 20\delta$) in a Mach 5 supersonic boundary layer.

Given the work to date, it is not clear if large-scale coherence, as has been documented in incompressible boundary layers, is a universal aspect in supersonic boundary layers. This issue is particularly important for understanding the mechanisms that drive the unsteadiness of shock-induced turbulent separation (Smits & Dussauge 1996). There is growing evidence that the large-scale unsteadiness of such flows is driven by low-frequency velocity fluctuations in the upstream boundary layer (Beresh, Clemens & Dolling 2002), and it is possible that large-scale coherent structures play a role in generating these fluctuations. Therefore, the aim of this work is to investigate the large-scale coherence in velocity fields in a supersonic (Mach 2) turbulent boundary layer. This was accomplished by using wide-field particle image velocimetry (PIV) in streamwise–spanwise planes to investigate the instantaneous flow structure and compute two-point correlations. The results are compared to incompressible and other supersonic turbulent boundary layer datasets.

M_∞	U_∞ (m s^{-1})	δ (mm)	δ^* (mm)	θ (mm)	u_τ (m s^{-1})	Re_θ ($U_\infty\theta/\nu_\infty$)	Re_τ ($u_\tau\delta/\nu_w$)
2	510	12.5	2.5	0.9	18.5	35000	5600

TABLE 1. Experimental parameters. M_∞ and U_∞ are free-stream Mach number and streamwise velocity, respectively. δ is the boundary layer thickness, δ^* is the displacement thickness, θ is the momentum deficit thickness and u_τ is the skin friction velocity.

2. Experimental setup and facilities

All of the experiments were performed in a Mach 2 blowdown tunnel at The University of Texas at Austin. The constant-area test section was 152 mm wide, 160 mm high and 760 mm long. The sidewalls of the test section were equipped with 19 mm thick fused silica windows of dimensions 152×51 mm^2 (length $\times$ height) to pass laser sheets. The top wall of the tunnel was fitted with a 19 mm thick acrylic window of size 205×65 mm^2 (length $\times$ width) for optical access. A total of about 4 m^3 of compressed air was provided by a Worthington HB4 four-stage compressor and stored in external tanks at a pressure of about 17250 kPa. The stagnation chamber pressure and temperature were approximately 261 ± 7 kPa and 292 ± 5 K, respectively. The measurements were made on the boundary layer that developed on the wall of the wind tunnel, approximately 0.5 m downstream of the nozzle exit. The boundary layer underwent natural transition and developed under approximately adiabatic wall temperature conditions. The mean properties of this boundary layer were characterized previously by Hou (2003) and table 1 lists relevant free-stream and boundary layer parameters.

Titanium dioxide (TiO_2) with a manufacturer-specified nominal particle diameter of 0.02 μm (actual size ≈ 0.2 μm) was used as seed particles for PIV (actual particle size was about 10 times larger than manufacturer specified size due to agglomeration). The particles were seeded upstream of the stagnation chamber of the tunnel by using a two-stage fluidized-bed seeder driven by compressed nitrogen followed by a cyclone separator. The Stokes number (St) of the particle is about 0.1 ($St = \tau_p/\tau_f$ with $\tau_p \approx 2.6$ μs the time scale of the particle and $\tau_f = \delta/U_\infty \approx 25$ μs a characteristic flow time scale). Samimy & Lele (1991) suggested that for particles to faithfully track the velocity fluctuations in a turbulent mixing layer, the Stokes number must be less than about 0.5. The seed particles were illuminated by pulsed laser sheets (thickness ~ 1 mm) from a pair of flashlamp pumped Nd:YAG lasers (Spectra Physics PIV 400) directed through one side window and oriented parallel to the tunnel floor as shown in figure 1. Sets of digital images were captured by two Kodak Megaplus CCD cameras (1024×1024 pixels) lined up next to each other in the streamwise direction as shown in figure 1 to provide a wide field of view whose area was approximately 100×50 mm^2. Nikon Nikkor 50 mm f/1.2 lenses were used with both cameras. The physical size of the cameras impeded the normal view of each camera to achieve the required continuous field of view. Therefore the cameras were oriented at a small angle ($< 10^\circ$) to get a spatially continuous field of view. The geometric distortion resulting from the perspective view was corrected in post-processing. This correction scheme enabled the correction of the in-plane velocity and coordinates only; however, part of the out-of-plane component is present in the streamwise velocity component and therefore results in marginally higher mean and r.m.s. values. Comparison of the mean values of the streamwise velocity with Hou (2003) (who measured velocities in streamwise–wall-normal planes using PIV in the same wind tunnel) indicates a difference of approximately 8 %. Data were acquired at two wall-normal locations,

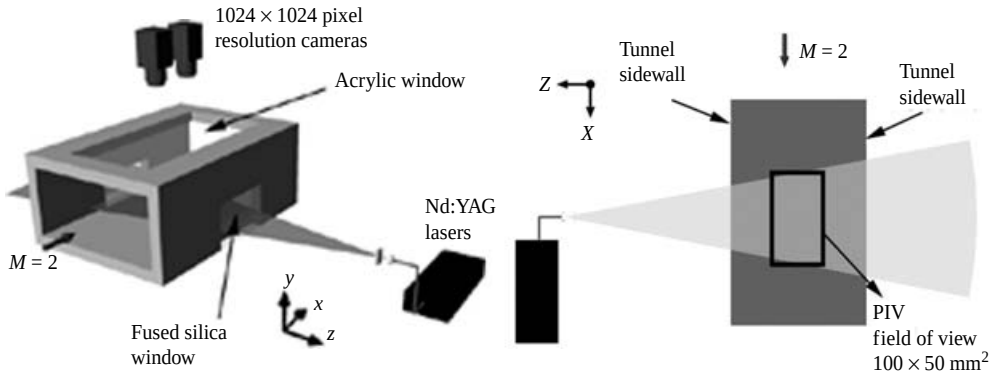

FIGURE 1. Experimental setup: (*a*) perspective view and (*b*) plan view.

y/δ	y^+	$\overline{U}^+$	σ_u^+	σ_w^+
0.16	900	24.2	1.76	0.92
0.45	2500	26.8	1.62	0.82

TABLE 2. Ensemble-averaged flow statistics. σ_u^+ and σ_w^+ are the r.m.s. values of the streamwise and spanwise velocity fluctuations normalized by u_τ and ρ/ρ_w.

$y/\delta = 0.16$ ($y^+ = 900$) and $y/\delta = 0.45$ ($y^+ = 2500$). A total of 600 images were acquired at each station for statistical convergence of mean and r.m.s. statistics of the velocity components.

The PIV images were processed using in-house Matlab-based software (a modified version of StanPIV or PIVlab obtained from Dr M. G. Mungal, Stanford University). The PIV code uses an adaptive window offset method and it was modified to utilize the central difference interrogation technique outlined in Wereley & Meinhart (2001), which recursively refines the interrogation window down to a size of 32×32 pixels. The linear resolution per interrogation window is 1.58 mm (0.12δ). A 50 % overlap was used to provide a vector field of size 128×64 vectors. Since the goal of this study is to resolve the large-scale features of the boundary layer this linear resolution was satisfactory. However, this resolution cannot be used to accurately measure statistics of gradient quantities like vorticity or to identify small-scale vortex cores in the flow field. This resolution is akin to a low-pass-filtered velocity field where the emphasis is on the large-scale structures. The average pixel displacement in the streamwise direction was 9 pixels. The vector fields were validated using a Gaussian engine that removed vectors with values outside 4 standard deviations from the mean. Any missing vectors were interpolated using a 3×3 local mean technique. The number of spurious vectors was less than 6% in the dataset.

The values of mean and r.m.s. statistics of the streamwise and spanwise velocity computed from the PIV data at each wall-normal location are shown in table 2. The r.m.s. of the velocity fluctuations was scaled according to Morkovin's hypothesis. The local density was calculated assuming a constant mean pressure across the boundary layer and mean local temperature (T) computed with the Crocco–Busemann relation $C_pT = C_pT_\infty + 0.5(U_\infty^2 - \overline{U}^2)$ (where C_p is the specific heat at constant pressure and $\overline{U}$ is the local mean streamwise velocity). The scaled values compare well with

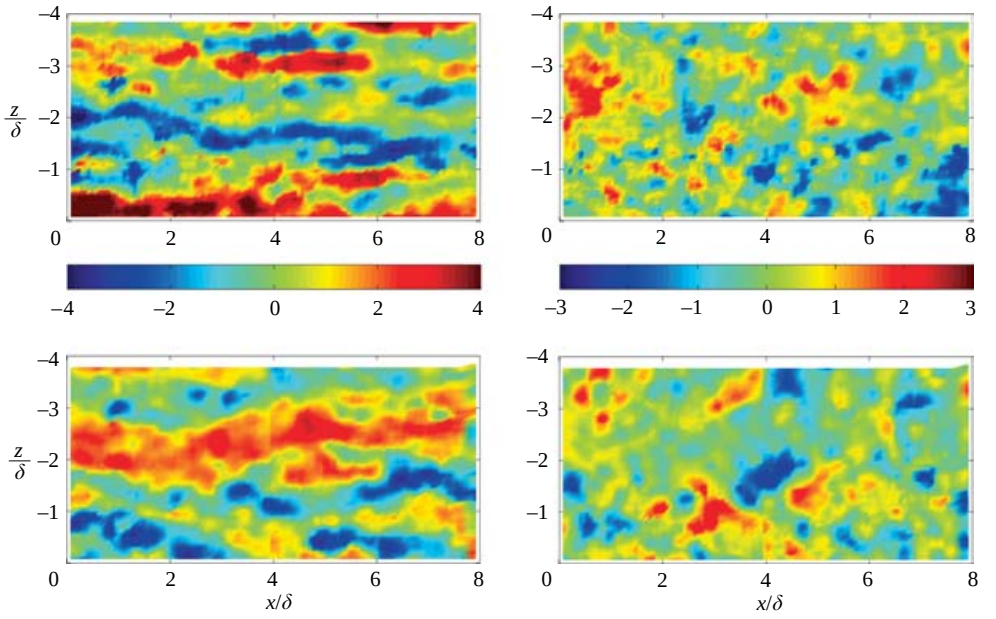

FIGURE 2. Streamwise and spanwise velocity fluctuations normalized by u_τ. (*a*) u/u_τ and (*b*) w/u_τ at $y/\delta = 0.16$, (*c*) u/u_τ and (*d*) w/u_τ at $y/\delta = 0.45$. The flow is from left to right.

previous incompressible and supersonic boundary layer data in the literature (Elena & Lacharme 1988; Smits & Dussauge 1996; Adrian *et al.* 2000).

3. Results and discussion

3.1. *Instantaneous structure*

Figure 2 shows typical wide-field plots of the instantaneous velocity fluctuations (u and w) at $y = 0.16\delta$ ($y^+ = 900$) and 0.45δ ($y^+ = 2500$). In the figure the flow is from left to right and the velocity fluctuations are scaled with skin friction velocity (u_τ). Note that the contour plots shown in figure 2 are from individual realizations, but the patterns are representative of those found in many fields.

The streamwise velocity fluctuation (u) plot shown in figure 2(*a*) reveals the existence of strips of uniform positive and negative fluctuations. These strips exhibit characteristic widths of approximately $0.25\delta - 0.5\delta$ and they extend a large distance in the streamwise direction. The streamwise extent of these coherent regions is at least 8δ. Other instantaneous fields also indicate that these long regions extend beyond the full field of view (i.e. $> 8\delta$). The strips also exhibit a spanwise gradient in u that is relatively large as the velocity changes by about $200\,\mathrm{m\,s^{-1}}(0.45U_\infty)$ over a distance of half a boundary layer thickness (i.e. 6 mm). It should be emphasized that these long structures are randomly distributed in space (i.e. not stationary) as they disappear when several vector fields are averaged.

Figure 2(*b*) is a plot of the spanwise velocity fluctuation (w) at $y/\delta = 0.16$. These fluctuations are in the range $\pm 3u_\tau$. This plot reveals that spanwise velocity is far less coherent along both the streamwise and spanwise directions. It also shows that w is mostly short, compact and seems to appear in spanwise patches of alternating positive and negative fluctuations.

Figure 2(*c*) is a plot of u at $y = 0.45\delta$ ($y^+ = 2500$). The overall structure at this location is similar to the lower wall-normal location; however, the spanwise scales are larger. Visual comparison of the instantaneous velocity fields indicates that the coherent regions of positive and negative u are wider in the spanwise direction and are at least as long in the streamwise direction compared to $y/\delta = 0.16$. Figure 2(*c*) reveals an instance where a coherent region is at least 8δ long and has a width of approximately δ. Figure 2(*d*) shows a plot of w at $y/\delta = 0.45$. It indicates that w is more compact than u, but the w fluctuations are longer and wider farther from the wall. This suggests an increasing trend in the representative length scale of the spanwise velocity in both streamwise and spanwise directions.

The presence of long streamwise structures is in agreement with the instantaneous visualization experiments of Samimy *et al.* (1994), where the upper part of the boundary layer ($y/\delta = 0.49$ and 0.65) was seen to be populated with elongated longitudinal structures. As noted previously, however, the $x-z$-plane visualizations obtained by Smith *et al.* (1989) and Smith & Smits (1995) in a Mach 2.5 boundary layer do not seem to support the presence of such elongated structures. The current results are consistent with those of Ünalmis & Dolling (1998) who made measurements of fluctuating wall and Pitot pressures in a Mach 5 turbulent boundary layer that developed on the wind tunnel wall. They computed cross-correlations of the pressure data and concluded that the boundary layer exhibits streamwise vortical structures. They interpreted these structures as probably resulting from Görtler-type vortices generated in the upstream nozzle. It is not known at this time whether the structures observed in figure 2 are remnants of a Görtler instability, but some evidence suggests they may not be. For example, it might be expected that Görtler vortices would exhibit vorticity that is primarily streamwise, in which case the contours of w should also exhibit the presence of elongated structures with alternating positive and negative spanwise velocity.

The patterns observed in figure 2 seem to be more consistent with the velocity fields from instantaneous PIV measurements made in incompressible boundary layers by Ganapathisubramani *et al.* (2003) and Tomkins & Adrian (2003). Both studies used the 'hairpin packet' model to explain the existence of instantaneous uniform-momentum zones. The region between the legs of the hairpin vortices contains negative velocity fluctuations and the zones on either side of the legs have positive velocity fluctuations (this is analogous to 'ejections' between the legs and 'sweeps' on either side of the legs). Adrian *et al.* (2000) hypothesized that 'hairpin packets' can contain up to 10 individual vortices propagating as a coherent entity that extends to streamwise distances greater than 2δ. However, hot-wire-based studies by Kim & Adrian (1999) and Hutchins, Ganapathisubramani & Marusic (2004) showed that these uniform-momentum regions extended to much larger streamwise distances ($> 15\delta$). Therefore, Kim & Adrian (1999) proposed a model for these very large-scale motions (VLSM) based on the 'hairpin packet' model. In this model hairpin packets group together to form a larger-scale structure as shown in figure 3.

Kim & Adrian (1999) also noted that the VLSM model is a hypothesis that avoids asserting that the observed large-scale coherence constitutes a new type of turbulent motion and simply uses the existing hairpin packet model as a basic building block. Since it is hypothesized in this model that a group of hairpin packets are convected together, the streamwise velocity fluctuations within such a group would have similar magnitudes and can be observed as uniform low- and high-speed regions in an instantaneous velocity field. The above-mentioned signature is remarkably similar to the patterns found in figure 2. Therefore, the VLSM model could be used to

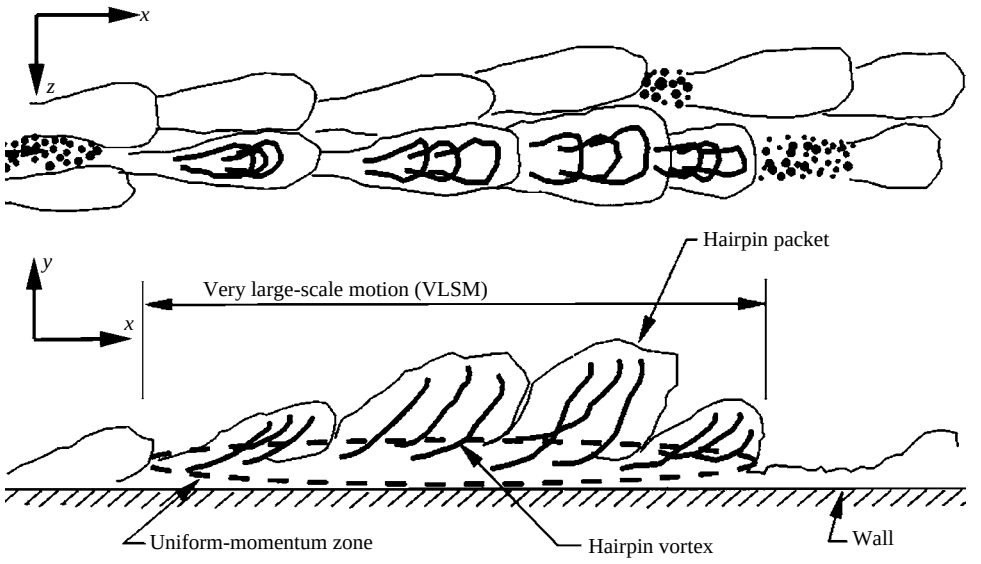

FIGURE 3. Schematic of a very large-scale motion (VLSM) model. Reused with permission from K. C. Kim and R. J. Adrian, *Physics of Fluids*, vol. 11, p. 417 (1999). Copyright 1999, American Institute of Physics.

understand the instantaneous flow patterns observed in the supersonic boundary layer. However, it should be noted that the spatial resolution of this study is not fine enough to capture the features of individual vortex cores, although it is sufficient to study the properties of the larger features like the elongated uniform-momentum zones.

3.2. *Statistical analysis*

Two-point correlations of velocity fluctuations were computed to confirm the validity of the qualitative observations made, based on instantaneous fields. The datasets in the two wall-normal locations enable the calculation of direct spatial correlations of the velocity components in a supersonic boundary layer without relying on Taylor's hypothesis to provide the streamwise extent of the correlations. The correlations were computed utilizing all vector fields at a given wall-normal position.

Figure 4(a, b) shows the two-point autocorrelations R_{uu} at $y/\delta = 0.16$ and 0.45. For $y/\delta = 0.16$, there is significant spatial coherence in the streamwise direction such that the correlation coefficient falls to a value of about 0.1 at a distance of 5δ. The equivalent plot at $y/\delta = 0.45$ is longer, with the value of R_{uu} equal to 0.25 at 5δ. The long negative correlation outboard of the positive correlation region supports the notion of adjacent low- and high-speed zones extending in the streamwise direction as seen in figure 2 in both wall-normal locations. This result is entirely consistent with a hairpin vortex packet model (proposed by Adrian *et al.* 2000), where hairpin vortices induce negative velocity fluctuations between their legs and positive fluctuations on either side of their legs. Note that the hairpin packets include a range of vortical structures including quasi-streamwise vortices/arches/horseshoes (Robinson 1991) and it is beyond the scope of this study to identify and isolate the properties of individual vortex cores.

At $y/\delta = 0.16$, the spanwise width of positive R_{uu} correlation is about 0.5δ. R_{uu} is marginally wider at $y/\delta = 0.45$. This is consistent with the results of two-point correlations in incompressible boundary layers computed by Kovasznay *et al.* (1970), Tomkins & Adrian (2003) and Ganapathisubramani *et al.* (2005). This is also

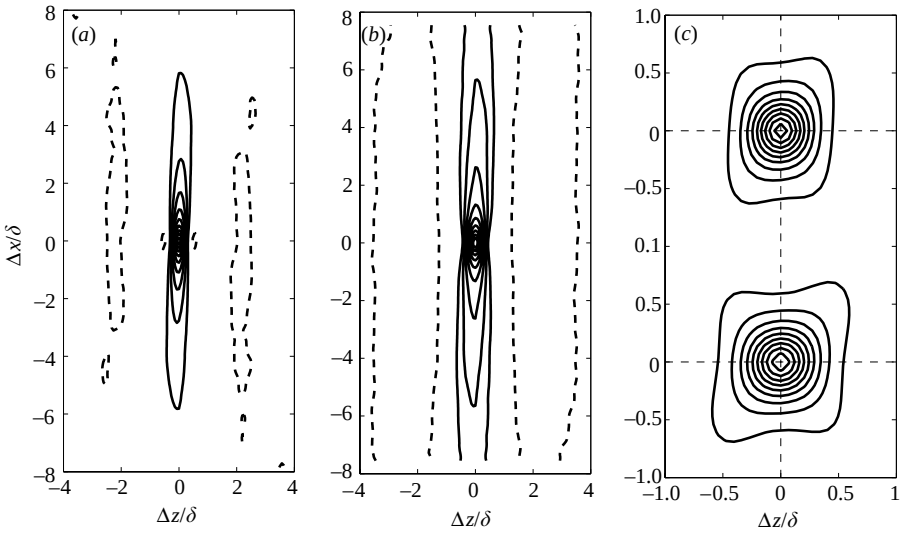

FIGURE 4. (a, b) Streamwise velocity autocorrelation R_{uu} at (a) $y/\delta = 0.16$, (b) 0.45. (c) Spanwise velocity autocorrelation R_{ww} at $y/\delta = 0.16$ (upper) and 0.45 (lower). The contour levels range from −0.1 to 1 in increments of 0.1 with negative levels shown with dotted lines. The zero contour is not shown.

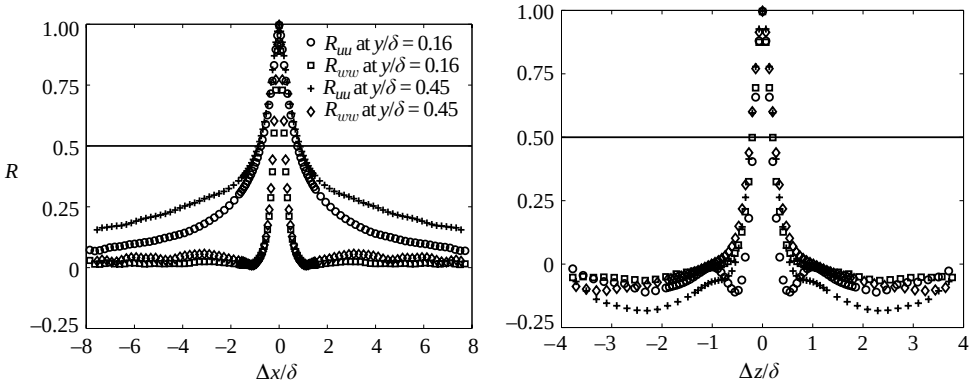

FIGURE 5. Velocity fluctuation autocorrelation functions at $y/\delta = 0.16$ and 0.45 along (a) $\Delta z = 0$ and (b) $\Delta x = 0$.

consistent with correlations computed in a Mach 3 supersonic boundary layer by Smits *et al.* (1989). The spanwise extent of the correlations demonstrates that typical flow structures increase in width with increasing wall-normal distance.

As shown in figure 4(c), the R_{ww} correlations in both wall-normal locations are compact in both streamwise and spanwise directions, indicating that the spanwise fluctuations are localized and do not possess an extended streamwise or spanwise coherence across the boundary layer. There is a small increase in the spanwise extent of R_{ww} correlations away from the wall as seen in figure 4(c). This increase could be attributed to the increase in geometric size of the representative average vortex structure.

In figure 5, the R_{uu} and R_{ww} correlations at $y/\delta = 0.16$ are compared with R_{uu} and R_{ww} at $y/\delta = 0.45$ along $\Delta z = 0$ and $\Delta x = 0$. These correlations are similar to those

obtained from point measurement techniques such as hot wires and LDV. However, this gives a direct spatial extent without relying on Taylor's hypothesis. First, note that the R_{ww} correlation drops very sharply, suggesting that the streamwise coherence in w is typically quite short. The R_{uu} correlation extends beyond the streamwise range examined, clearly indicating the presence of coherent streamwise regions longer than 8δ. The short compact R_{ww} could represent a smaller scale structure (like an individual vortex core) and the long R_{uu} represents a larger coherence. The above observations are consistent with the VLSM model.

To examine the correlations further, a contour level of R (say 0.5) is chosen to define a representative length scale (λ) such that $\lambda = 2\Delta$ at $R = 0.5$ (i.e. full width of the correlation function at half the maximum value). The length-scale λ can be computed using both R_{uu} and R_{ww} in both the x- and z-directions. The length scales computed based on the correlations would reveal a representative scale of coherence in both streamwise and spanwise directions. The length scales deduced represent an average spatial coherence that include both low- and high-speed zones.

It must be noted that the coarse resolution of the velocity fields has an impact on the length scales deduced from the two-point correlations. A recent study by Spencer & Hollis (2005) suggests that the integral length scale and the r.m.s. velocity fluctuations can be deduced to within 10 % uncertainty for a resolution that is 5 times smaller than the true integral length scale. The accuracy is better for datasets with better resolution. In this study, the resolution is approximately 5 times smaller than the spanwise integral length scale based on R_{uu} (λ_z^u) and over 10 times smaller than the streamwise integral length scale (λ_x^u). Therefore the reader must be aware that the values of λ reported in this paper have a maximum uncertainty of approximately 10 %.

The streamwise length scale based on R_{uu}, λ_x^u has values of 1.51δ and 1.73δ at $y/\delta = 0.16$ and 0.45 respectively. The length scales found are at least 4 times larger than the λ_x^u computed for the same contour level in an incompressible boundary layer by Ganapathisubramani *et al.* (2005) at $Re_\theta = 2500$. It is possible that this difference in scale is due to compressibility or Reynolds number effects as will be discussed below.

Ganapathisubramani *et al.* (2005) suggested an increasing trend in the streamwise length scale through the logarithmic region of the boundary layer. The mean velocity profiles for the current boundary layer (as measured using PIV by Hou 2003) indicate that the two wall-normal locations are in fact in the logarithmic region of the boundary layer when scaled with u_τ and ν_w. The mean velocity profile was found to follow the logarithmic line until $y^+ = 3000$ ($y/\delta = 0.5$). The log region seems to extend farther in the wall-normal direction in supersonic boundary layers ($y/\delta \leqslant 0.6$, see also Robinson 1986; Kistler 1959 and other mean velocity profiles in Smits & Dussauge 1996) than in incompressible ones ($y/\delta \leqslant 0.3$). This feature may make the supersonic boundary layer behave more like an incompressible channel or pipe flow, because these latter flows exhibit extended logarithmic regions (the log region extends almost across the entire channel half-width). Furthermore, Christensen *et al.* (2004) and Kim & Adrian (1999) computed length scales in an incompressible channel flow and pipe flow, respectively, and found an increasing trend in the streamwise extent through the outer region (i.e. until $y = 0.6h$, where h is channel half-width or pipe radius). Both studies found that the streamwise length scale started decreasing beyond $y = 0.6h$. Christensen *et al.* (2004) also found an increasing trend in the streamwise extent of the R_{uu} correlation with Reynolds number. The results from the present study are consistent with the findings of both Christensen *et al.* (2004) and Kim & Adrian (1999). The scaling of the streamwise length scales based on R_{uu} is not well

understood. The outer variable (δ) was chosen as the scaling parameter in this study to remain consistent with previous studies in the literature. However, there is some evidence in the literature that λ_x^u scales with δ for higher Reynolds numbers in incompressible boundary layers (see Marusic & Hutchins 2005).

It is worth noting that streamwise length scales computed based on correlations in the present study are in contrast with the hot-wire-based findings of Smits *et al.* (1989). They computed length scales from autocorrelations of mass-flux fluctuations and found a decreasing trend in the length scales with increasing wall-normal distance in the locations examined in their study of a Mach 2.9 boundary layer ($y/\delta = 0.2$, 0.51 and 0.82; the logarithmic region in this study seems to extend to $y/\delta \approx 0.5$, see Spina 1988). Also, the length scales found in the present study are much larger than the lengths found in Smits *et al.* (1989) for similar contour levels at comparable wall-normal locations (at least 2–3-times larger). The reasons behind this wide disparity in the streamwise length scales is not known. However, there is good agreement between the studies in the spanwise scales computed based on the correlations.

The spanwise length scale based on R_{uu}, λ_z^u, is 0.36δ and 0.48δ for $y/\delta = 0.16$ and 0.45 respectively. This indicates an increase in the spanwise length scale as observed by various other researchers in both supersonic and incompressible boundary layers (Smits & Dussauge 1996; Tomkins & Adrian 2003; Ganapathisubramani *et al.* 2005). The values of λ_z^u computed in this study seem to collapse with spanwise length scales obtained from other studies (in both incompressible and supersonic boundary layers) when scaled with outer variables (δ). This outer scaling is consistent with the findings of Mclean (1990) and Werk, Naguib & Robinson (1991) in incompressible boundary layers, where it was found that the outer-scaled spanwise length scales collapsed for higher Reynolds numbers across the boundary layer.

4. Conclusions

In this paper, results of wide-field PIV measurements in streamwise–spanwise planes of a Mach 2 supersonic turbulent boundary layer are presented. Some of the key conclusions from examining the instantaneous velocity fields and two-point correlation data are:

(i) Instantaneous streamwise velocity fields at $y/\delta = 0.16$ and 0.45 reveal the presence of strips of low- and high-speed fluid that are coherent over large streamwise distances. These long coherent regions appear compact in the spanwise direction with width approximately equal to δ at both wall-normal locations. The signature of the coherent zones is consistent with the VLSM model where spatial organization of multiple hairpin packets leads to long streamwise coherence as proposed by Kim & Adrian (1999).

(ii) Two-point velocity correlations were computed and contours of R_{uu} reveal long tails at both wall-normal locations, suggesting that instantaneous structures with long streamwise coherence are a frequent occurrence. Contours of R_{ww} are compact in both streamwise and spanwise directions, indicating a representative scale of individual vortex cores.

(iii) The correlation data also seem to indicate an increase in the streamwise length scale (λ_x^u) between $y/\delta = 0.16$ and 0.45, suggesting an increasing trend in length scale in the logarithmic region (noted by other researchers in incompressible boundary layers). The spanwise length scale (λ_z^u) reveals a marginally increasing trend with wall-normal distance and is consistent with the spanwise-scale growth found in other studies in both incompressible and supersonic boundary layers.

(iv) The presence of these long streamwise coherent velocity fluctuations could be the source of low-frequency unsteadiness of the separated flow observed in various shock wave–turbulent boundary layer interaction studies.

The authors wish to thank Pablo Bueno, Edward J. Zihlman Jr and Venkateswaran Narayanaswamy for all the help in the data acquisition phase of the study. The authors would also like to thank the reviewers and the editor for their comments which helped improve the contents of the paper. The authors gratefully acknowledge the support of the Air Force Office of Scientific Research under grant FA9550-04-1-0387 and of the Army Research Office under grant DAAD19-03-1-0178.

REFERENCES

Adrian, R. J., Meinhart, C. D. & Tomkins, C. D. 2000 Vortex organization in the outer region of the turbulent boundary layer. *J. Fluid Mech.* **422**, 1–53.

Beresh, S. J., Clemens, N. T. & Dolling, D. S. 2002 Relationship between upstream turbulent boundary-layer velocity fluctuations and separation shock unsteadiness. *AIAA J.* **40**, 2412–2422.

Bogard, D. G. & Tiederman, W. G. 1986 Burst detection with single-point velocity measurements. *J. Fluid Mech.* **162**, 389–413.

Christensen, K. T., Wu, Y., Adrian, R. J. & Lai, W. 2004 Statistical imprints of structure in wall turbulence. *AIAA Paper 2004-1116*.

Elena, M. & Lacharme, J. P. 1988 Experimental study of a supersonic turbulent boundary layer using a laser doppler anemometer. *J. Theor. Appl. Mech.* **7**, 175–190.

Ganapathisubramani, B., Hutchins, N., Hambleton, W. T., Longmire, E. K. & Marusic, I. 2005 Investigation of large-scale coherence in a turbulent boundary layer using two-point correlations. *J. Fluid Mech.* **524**, 57–80.

Ganapathisubramani, B., Longmire, E. K. & Marusic, I. 2003 Characteristics of vortex packets in turbulent boundary layers. *J. Fluid Mech.* **478**, 35–46.

Garg, S. & Settles, G. 1998 Measurements of a supersonic turbulent boundary layer by focusing schlieren deflectometry. *Exps. Fluids* **25**, 254–264.

Head, M. R. & Bandyopadhyay, P. 1981 New aspects of turbulent boundary-layer structure. *J. Fluid Mech.* **107**, 297–337.

Hou, Y. X. 2003 Particle image velocimetry study of shock induced turbulent boundary layer separation. PhD thesis, Department of Aerospace Engineering and Engineering Mechanics, The University of Texas at Austin.

Hutchins, N., Ganapathisubramani, B. & Marusic, I. 2004 Dominant spanwise Fourier modes and existence of very large scale coherence in turbulent boundary layers. In *15th Australasian Fluid Mechanics Conference, December 13–17, Sydney, Australia*.

Kim, K. C. & Adrian, R. J. 1999 Very large-scale motion in the outer layer. *Phys. Fluids* **11**, 417–422.

Kistler, A. L. 1959 Fluctuation measurements in supersonic turbulent boundary layer. *Phys. Fluids* **2**, 290–296.

Kovasznay, L. S. G., Kibens, V. & Blackwelder, R. F. 1970 Large-scale motion in the intermittent region of a turbulent boundary layer. *J. Fluid Mech.* **41**, 283–326.

Mclean, I. R. 1990 Near-wall eddy structure in an equilibrium turbulent boundary layer. PhD thesis, University of Southern California.

Marusic, I. & Hutchins, N. 2005 Evidence of very long meandering structures in the logarithmic region of turbulent boundary layers. *J. Fluid Mech.* (under review).

Morkovin, M. V. 1962 Effects of compressibility on turbulent flows. In *Mecanique de la Turbulence*, pp. 367–380. CNRS.

Owen, F. K. & Horstmann, C. C. 1972 On the structure of hypersonic turbulent boundary layers. *J. Fluid Mech.* **53**, 611–636.

Panton, R. L. 1997 *Self-Sustaining Mechanisms of Wall Turbulence*. Comp. Mech. Publications.

Robinson, S. K. 1986 Space-time correlation measurements in a compressible turbulent boundary layer. *AIAA Paper* 1986-1130.

Robinson, S. K. 1991 Coherent motions in turbulent boundary layers. *Annu. Rev. Fluid Mech.* **23**, 601–639.

Samimy, M., Arnette, S. A. & Elliot, G. S. 1994 Streamwise structures in a supersonic turbulent boundary layer. *Phys. Fluids* **6**, 1081–1083.

Samimy, M. & Lele, S. K. 1991 Motion of particles with inertia in a compressible free shear layer. *Phys. Fluids* A **3**, 1915–1923.

Smith, M. W. & Smits, A. J. 1995 Visualization of the structure of supersonic turbulent boundary layers. *Exps. Fluids* **18**, 288–302.

Smith, M. W., Smits, A. J. & Miles, R. B. 1989 Compressible boundary layer density cross section by uv rayleigh scattering. *Opt. Lett.* **14**(17), 916.

Smits, A. J. & Dussauge, J. P. 1996 *Turbulent Shear Layers in Supersonic Flow*. American Institute of Physics Press.

Smits, A. J., Spina, E. F., Alving, A. E., Smith, R. W., Fernando, E. M. & Donovan, J. F. 1989 A comparison of the turbulence structure of subsonic and supersonic boundary layers. *Phys. Fluids* A **1**, 1865–1875.

Spencer, A. & Hollis, D. 2005 Correcting for sub-grid filtering effects in particle image velocimetry data. *Meas. Sci. Technol.* **40**, 2323–2335.

Spina, E. F. 1988 Organized structures in a supersonic turbulent boundary layer. PhD thesis, Princeton University.

Theodorsen, T. 1952 Mechanism of turbulence. In *Proc Second Midwestern Conference on Fluid Mechanics*. Ohio State University, Columbus, Ohio, USA.

Tomkins, C. D. & Adrian, R. J. 2003 Spanwise structure and scale growth in turbulent boundary layers. *J. Fluid Mech.* **490**, 37–74.

Ünalmis, O. H. & Dolling, D. S. 1998 Experimental study of causes of unsteadiness of shock induced turbulent separation. *AIAA J.* **36**, 371–378.

Wereley, S. T. & Meinhart, C. D. 2001 Second-order accurate particle image velocimetry. *Exps. Fluids* **31**, 258–268.

Werk, C. E., Naguib, A. M. & Robinson, S. K. 1991 Scaling of spanwise length scale in a turbulent boundary layer. *AIAA Paper* 1991-0235.